Journal of Coastal Research	4	1	115-128	Charlottesville, Virginia	Winter 1988

A STUDY ON NEARSHORE BAR DYNAMICS IN A LOW-ENERGY ENVIRONMENT; NORTHERN ZEALAND, DENMARK.

Troels Aagaard

Institute of Geography
University of Copenhagen
Øster Voldgade 10
DK-1350 Copenhagen K, Denmark

ABSTRACT

AAGAARD, T., 1988. A Study on Nearshore Bar Dynamics in a Low-Energy Environment; Northern Zealand, Denmark. *Journal of Coastal Research*, 4(1), 115-128. Charlottesville, ISSN 0749-0208.

Rhythmic bar movements have been investigated in a low- energy environment. During sporadic high-energy events the two innermost bars moved seaward and again shoreward when conditions became calmer. In very calm periods, the bars were arrested in position. Bar dimensions have been compared to the structure of standing infragravity edge waves to test the hypothesis that these waves control the shape and formation of the bars. In the main, edge wave periods calculated from the rhythmic pattern conformed well with those calculated from the bar distance to shore, especially after a major storm. Other hypotheses of bar formation have been evaluated, but it was found that standing edge waves may be a predominant parameter in the formation and position of bars.

ADDITIONAL INDEX WORDS: *Rhythmic bars, bar migration, bar genesis, morphodynamics, edge waves*

INTRODUCTION

Despite nearshore bars being an extensively studied phenomenon, no universally accepted model for their formation and migration has yet been formulated. Partly this is due to the fact that bars show greatest mobility during storms, when detailed field work is a difficult task. Furthermore, several factors may contribute to their dynamics. Nearshore bars may occur in a broad spectrum of forms ranging from parallel (linear) to crescentic, or they may be situated *en echelon,* forming a greater or lesser angle with the shoreline (transverse bars). Commonly a relation has been observed between number of bars and nearshore gradient; a shallow beach normally contains more bars than a steep beach (EVANS, 1940; KOMAR, 1976). As a rule, bar size and spacing between bars increase seaward (*e.g.* SAYLOR and HANDS, 1970; EXON, 1975; GREENWOOD and SHERMAN, 1984). The direction of migration is normally associated with the energy level; with a falling energy level the bars migrate shoreward and vice versa (*e.g.* HAYES, 1972; WINANT *et al.* , 1975; SHORT, 1979; SALLENGER *et al.* , 1985). A model for the migration and development of bars was presented by WRIGHT *et al.* (1979) and SHORT (1979). In this model, the inner bar migrates shoreward with a change of form from linear to crescentic and transverse during a falling energy level after a storm; the bar finally merges with the foreshore as a low-tide terrace or a berm. Along protected Danish coasts, the wave climate is extremely variable. Relatively high energy events of short duration alternate with very low energy conditions. Therefore, the above-mentioned sequence rarely reaches the final reflective beach stage. On the contrary, arrested forms, *i.e.* forms being out of equilibrium with the prevailing energy level, may occur. These greatly varying energy levels are due to a short fetch and frequent cyclone passages creating intense storms.

In this paper, a field study on bar dynamics is reported. Special attention is given to a very intense storm on September 6, 1985. Some hypotheses on bar formation are discussed, and the possibility of a causal relation between

87007 received 10 February 1987; accepted in revision 14 April 1987.

infragravity standing waves and bar location is examined.

BAR FORMATION AND MIGRATION

Several hypotheses concerning bar formation and migration have been advanced, a number of which will be outlined in this section.

EVANS (1940) and MILLER (1976) thought that bar formation was due to vortex action at the breakpoint of plunging breakers. In this model, the vortex excavates a trough while the eroded sediment is being transported seaward forming a bar. A series of breaker zones generates a series of bars, each bar representing the average breakpoint position for waves of a certain size. The bars migrate when the breakpoint positions change. Spilling breakers do not cause bar formation, as the vortex is much smaller and limited to the upper parts of the water column.

Another hypothesis was put forward by KING and WILLIAMS (1949). According to their model, bars are being formed by shoreward sediment transport outside the breakpoint, along with a seaward directed transport inside the breakpoint leading to a convergence in the breaker zone (KING and WILLIAMS, 1949; INGLE, 1966; DYHR-NIELSEN and SØRENSEN, 1970; SVENDSEN, 1984). The shoreward directed transport outside the breakpoint is caused by the increasing wave asymmetry and resulting drift velocity at the bottom. At the breakpoint, the transport rate suddenly decreases and sediment is deposited. Inside the breakpoint, a seaward directed bottom current, commonly known as the undertow, has frequently been observed under spilling breakers (INGLE, 1966; SALLENGER *et al.* , 1983; WRIGHT *et al.* , 1982a). This current supposedly move sediment towards the breakpoint. If the wave is reformed in the trough, a renewed shoreward transport of sediment occurs under the unbroken wave. Thus a series of bars may be formed. Under fully dissipative conditions, where breakers are spilling throughout the surf zone, only one bar can exist (SVENDSEN, 1984).

A somewhat similar hypothesis was proposed by GREENWOOD and DAVIDSON-ARNOTT (1975, 1979) and GREENWOOD and HALE (1980). They concluded, in line with the convergence model, that sediment is transported landward by the shoaling waves outside the breakpoint. The transport rate decreases at the breakpoint leading to accumulation of sediment and bar formation. Sediment tending to infill the trough is transported away by the longshore current and led seaward by rip currents; this horizontally segregated flow should cause the formation of crescentic bars. The net current is shoreward over bar horns and seaward in bays. Sediment is continually being circulated through the bar without necessarily any net movement of the bar form; the bar is in a dynamic equilibrium. Bar dynamics and morphology is thus governed by the current circulation, which is believed to be topographically induced with feedback mechanisms between circulation and topography.

The final hypothesis reviewed here is based on the presence of infragravity waves, standing in the offshore direction. These waves may be either edge waves or leaky modes. Progressive edge waves or two-dimensional leaky mode standing waves might generate a linear bar, while edge waves standing in the longshore direction, having a well-defined longshore length scale, might contribute to the formation of rhythmic bar topography (HOLMAN and BOWEN, 1982; BOWEN and HUNTLEY, 1984).

Zero-crossings of drift velocity occur at both nodes and antinodes in the boundary layer under cross-shore standing waves (CARTER *et al.* , 1973). Thus sediment will converge towards nodes or antinodes, but not both (SHORT, 1975). If the sediment is transported as bedload, the convergence will be towards nodes, while suspended sediment will converge towards antinodes. On an equilibrium profile where no sediment transport due to the incident waves is taking place, this equilibrium may be perturbed by other wave action, *e.g.* standing waves (BOWEN, 1980). The incident waves agitate the sediment, which may be transported by an even weak superimposed net current.

BOWEN (1980) suggested a model for the formation and position of linear bars involving leaky mode standing waves or high-mode progressive edge waves. The cross-shore structure of these wave motions is very much alike. The leaky mode wave structure is a function of J_0 (χ), where

$$\chi^2 = 4\omega^2 x/g \tan \beta \quad (1)$$

Table 1. *Values of χ^2 for which zero-crossings of drift velocity occur. Zero-crossings at antinodes and nodes of the wave form are defined as $Z_n^{(1)}$ and $Z_n^{(2)}$, respectively.*

	χ^2	
n	$Z_n^{(1)}$	$Z_n^{(2)}$
1	13.9	26.3
2	49.2	70.2
3	103	135
4	178	219
5	271	322

After BOWEN (1980).

J_o is the zero-order Bessel-function, χ a non-dimensional cross-shore length scale, ω is the radian frequency of the wave motion = $2\pi/T$, x is a length scale, and β the gradient of the nearshore. Zero-crossings of the drift velocity at 1 2 antinodes defined as $Z_n^{(1)}$, or nodes defined as $Z_n^{(2)}$ are given in Table 1. These zero-crossings occur at (eq. 1)

$$x_n = g \tan\beta \cdot Z_n^{(r)}/4\omega^2;\ r = 1, 2 \qquad (2)$$

Theoretically, the progressively increasing values of $Z_n^{(r)}$ signify, that bar spacing will increase in the offshore direction. If the distance from the shoreline to a given bar, x_n, is known, standing wave periods corresponding to this distance may be calculated from (eq.2)

$$T = 2\pi \left(\frac{4\, x_n}{g \tan\beta \cdot Z_n^{(r)}} \right)^{1/2} \qquad (3)$$

Wave periods corresponding to bar distances in nature are normally of infragravity frequencies.

BOWEN's model does not predict whether bars will be located at nodes or antinodes. WRIGHT *et al.* (1982b, 1986) found antinodes over the bar and nodes in the trough. KATOH (1984) found that suspended sediment converged towards antinodes of standing waves, thereby forming bars.

To induce a longshore rhythmicity in the bar form, at least two edge waves of the same frequency must exist. BOWEN and INMAN (1971) showed theoretically that two progressive edge waves of the same mode number moving in opposite directions, thus forming a standing edge wave, induce a rhythmicity in the drift velocity field at the bottom. They hypothesized that this zonation might give rise to the formation of crescen- tic bars. The zones of drift velocity convergence appear in crescentic bands. However, it may be that the ability of the edge waves in governing the cell circulation pattern is more significant for the development of rhythmic topography. WRIGHT *et al.* (1979, 1982b) found a shoreward directed net current over the bar horns where antinodes occurred, and rip currents at cross-shore nodes.

The wavelength of the rhythmic topography, λ, is given by

$$\lambda = L_e/2 \qquad (4)$$

where L_e is the edge wave wavelength,

$$L_e = (g/2\pi)\, T_e^2 \sin (2n+1)\beta \qquad (5)$$

(URSELL, 1952). T_e is the edge wave period and n is the mode number of the edge wave (*i.e.* the number of zero-crossings in the offshore direction). From eqs. (4) and (5), the edge wave period corresponding to a given morphological wavelength, λ, is therefore

$$T_e = \left(\frac{4\pi\lambda}{g \sin (2n+1)\beta} \right)^{1/2} \qquad (6)$$

STUDY AREA AND METHODS

The field work was conducted at Hald Strand at the north coast of Zealand from April through October 1985 (Figure 1). The amount of loose sediment in the area is limited, but as part of a beach nourishment test, about 25,000 m^3 of sand was fed to the beach during the summer of 1984. Four bars are present in the area, the two outermost ones with a very subdued relief. The gradient of the nearshore varies from 0. 019 in the western part of the area to 0. 016 in the central and eastern parts. The profiles exhibit a change of gradient at a depth of about 6 m (about 350 m from the shoreline), corresponding to the position of the trough between the two outermost bars, bars 3 and 4 (Figure 2). The study area is situated between two morainic promontories (Baunehöj and Galgebjerg). Abrasional platforms are associated with these headlands. The curvature of the

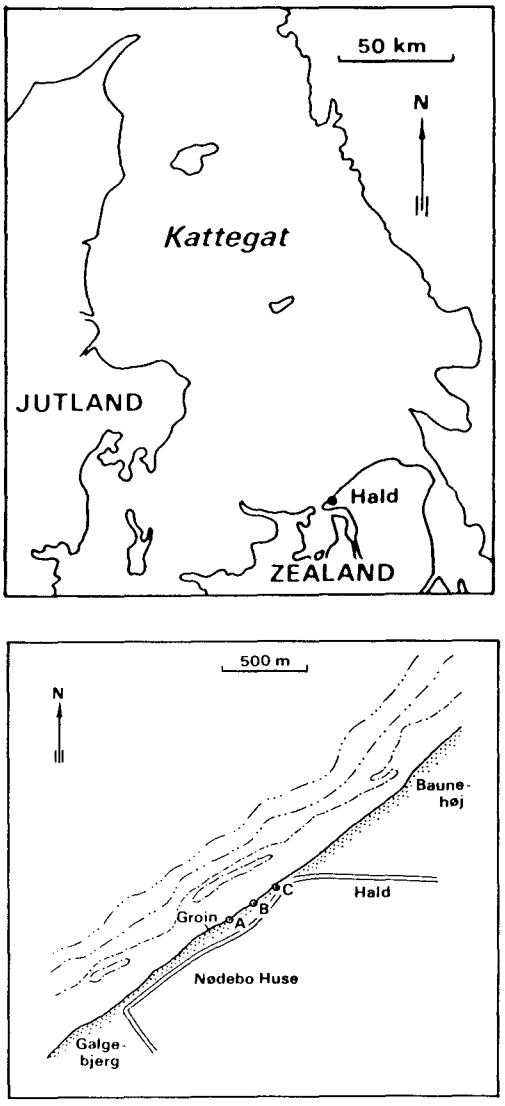

Figure 1. Location of the research area. Profiles were situated between points A and C.

coastline is, however, small. The composition of sediment is heterogenous. Fine sand with a mean grain size of about 0.14 mm forms a thin discontinuous layer over compact till, the till giving the seafloor an irregular appearance. Maximum fetch is about 90 nautical miles from the north, which precludes long period swell. Wave heights recorded at Kattegat South Light Vessel, situated some 25 nautical miles west of Hald, exceed 0.7 m for about 50% of the time. Representative wave periods are between 2 and 3 seconds. During a storm from the northwest, a breaker height of 2.5 m and a wave period of 6 seconds were observed. The tide is semidiurnal with a range of about 0.4 m. Due to the above-mentioned lack of loose sediments, it lies near at hand to believe that the area might be unsuitable for the study of bars. As a matter of fact, this deficit resulted in the bars occurring as ribbons of sand, simplifying identification in the field and on aerial photographs. The beach was surveyed about once a month and after each high-energy episode. The field work consisted of tachyometric beach surveys, using a theodolite fitted with an electro-optic range finder. Five profile lines, numbered 250-450, spaced at a distance of 50 metres apart, were extended seaward by echo-profiling.

Significant wave heights and wave periods were measured from a Waverider-buoy at a depth of about 7 m; breaker heights were measured or visually estimated. The Waverider was together with two Marsh-McBirney electromagnetic current meters deployed by the Danish Hydraulic Institute. These current meters were unfortunately withdrawn, while the Waverider was malfunctioning during the storm in September 1985. Water level was recorded at Hundested Harbour, 5 kilometres west of the study site. Bar distance from shore, and wavelength of the frequently occurring rhythmic topography were related to eqs. (3) and (6) for determination of standing wave periods, corresponding to these dimensions. Periods calculated from the two equations were compared. Bar distance from shore was measured at the central axis of the bar; for crescentic bars, these distances were measured in the bays, this scale being analogous to the linear bar case (SALLENGER *et al.* , 1985). The movements of bars 3 and 4 will not be analyzed, as these bars were only weakly developed and measurement errors were rather large this far from the shoreline.

RESULTS

During the survey period, the wave climate was very variable (Figure 3). When the Waverider was malfunctioning, wave heights were estimated from earlier or later recorded analogous climatic situations, or visually estimated. During these periods, wave heights are therefore only approximate. Incident wave energy

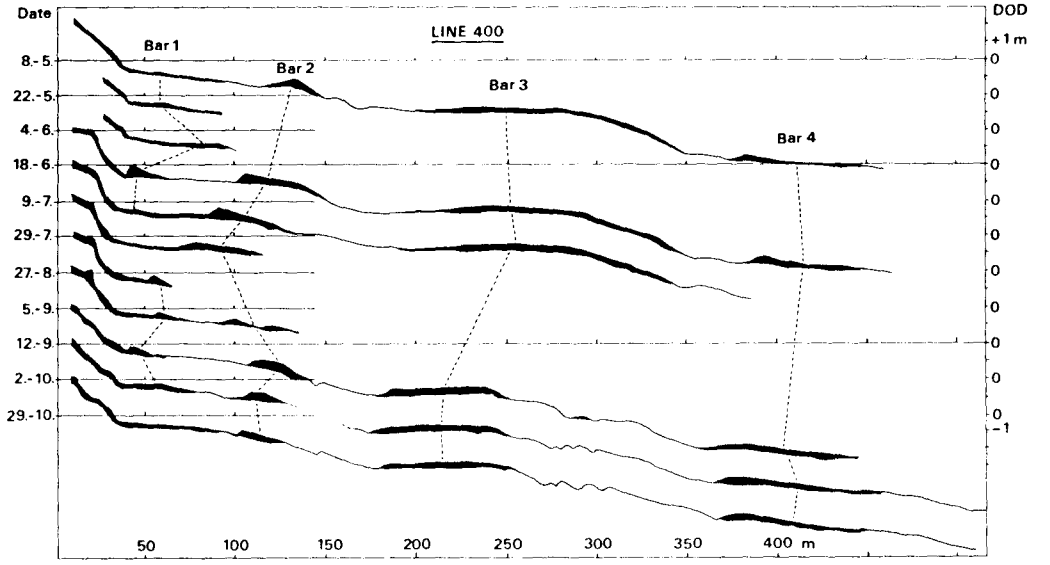

Figure 2. Stages in profile development; profile line 400. Dashed lines are drawn through bar axes. Thickness of the sand layer not to scale.

was generally low in the period May through August. Only occasionally did the wave height exceed 1 m. On September 6, a storm occurred in Kattegat. Wind speed reached 25 m/s from the northwest, *i.e.* a shore-normal wave incidence. The storm was associated with a surge, the water level reaching a maximum of 1. 16 m DOD (Danish Ordnance Datum). Estimated wave height exceeded 2 m for about 30 hours; in the late afternoon of September 6, visually estimated wave height was 2.5 m. On October 12, a storm of shorter duration and more westerly approach occurred. On this occasion, the maximum recorded significant wave height was 2.8 m. Wave periods were generally 2-3 seconds. A wave period of 6.0 seconds was observed on September 6, while a period of 5.6 seconds was recorded on October 12.

Bar Dynamics

The temporal migration of bars 1 and 2 is depicted on Figure 4. Considering bar 1, the direction and rate of migration shows great spatial and temporal variations. This is due to the presence of rhythmic topography, whose position and pattern changed between survey dates. Only twice, in the period 18/6-9/7 and in the beginning of September, an overall seaward migration of bar 1 was significant. The net migration of bar 1 over the entire study period was negligible (~ 1 m seaward). The bar oscillated around a mean position with small adjustments according to the prevailing wave climate. Movements of bar 2 are of a different nature. They are far more systematic, and the direction of migration is more or less the same in all profiles during a given interval between surveys. Part of the explanation may be the less frequent registration of bar position, and that the rhythmic amplitude as a rule is more subdued. But the result also indicates that bar 2 requires a higher energy level in order to move seaward. Bar 2 migrated shoreward throughout the summer. Not until the storms in September did it move seaward. Topographical maps of the study area on selected dates appear in Figure 5. The relief of bar 2, defined as the vertical distance from bar crest to baseline (Figure 6), shows a relation with the direction of migration. A seaward migration results in an increased relief, and vice versa. Water depth at bar base exhibits a significant spatial variation. The bars are situated at the greatest depth in the western part of the area (profile lines 250 and 300), where the nearshore gradient is the

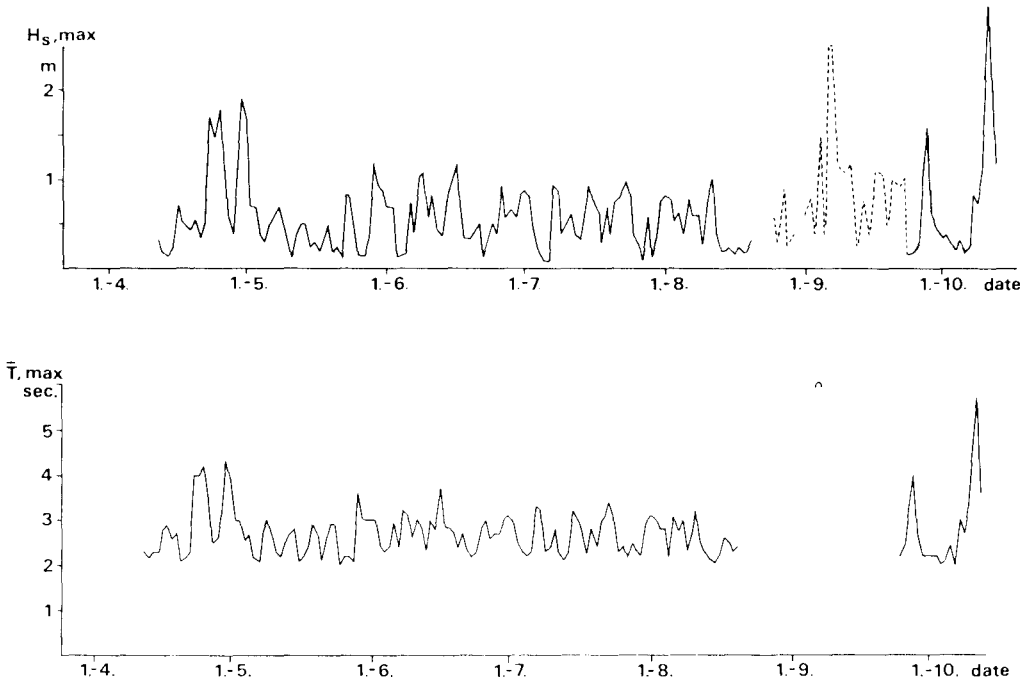

Figure 3. Variation of maximum daily significant wave height (a) and $\bar{T}$ (b) at Hald during the period April-October 1985. Dashed lines signify periods when Waverider-data are missing. Wave heights were then estimated from recorded similar meteorological situations 1984-1986, or alternatively visually estimated.

steepest (Figure 7). Also the bars are here farthest from shore. This indicates that there is no simple inverse relation between gradient and bar distance from shore, and that the bar is not situated at the same water depth along the coast, as might be expected were the bar position determined by the location of the breakpoint. Comparison of wave data and bar migration (Figure 3 and Table 2) indicates that bar 2 is able to move seaward under conditions with $H_s \geq 1.3$ m, although this is not invariably the case. During the period September 12 - October 2, wave heights reached the same level as between July 29 - September 5, but directions of migration were opposite. However, the shoreward migration before October 2 may be due to the bar having moved shoreward since the "high-energy" event on September 28. As regards bar 1, a similar analysis indicates that it may move seaward under conditions with $H_s \geq 0.9$ m. It must be stressed, however, that these values are only valid for this specific site, and that the data base is very small. A more thorough analysis of the relation between wave height and bar migration is hindered by periodically missing wave data and the infrequent surveys; the detailed migration between survey dates is not known.

Edge Wave Calculations.

In Table 3, hypothetical edge wave periods computed from morphological dimensions of bar 1 (eqs.3 and 6, with bars at antinodes) are compared. Twice, on July 29 and on October 2, a satisfactory correlation was found between periods calculated from the rhythmic wavelength (λ_1) and those calculated from bar distance to shore (x_1), these dimensions approximately corresponding to the structure of standing mode 1 edge waves with periods of 60 and 50 seconds, respectively. On two occasions (June 18 and July 9) bar 1 is somewhat too close to the shoreline in proportion to the rhythmic wavelength when a mode 1 edge wave is assumed. Prior to these dates, the most likely situations in which standing waves of low frequency might have occurred were of short duration, and the maxi-

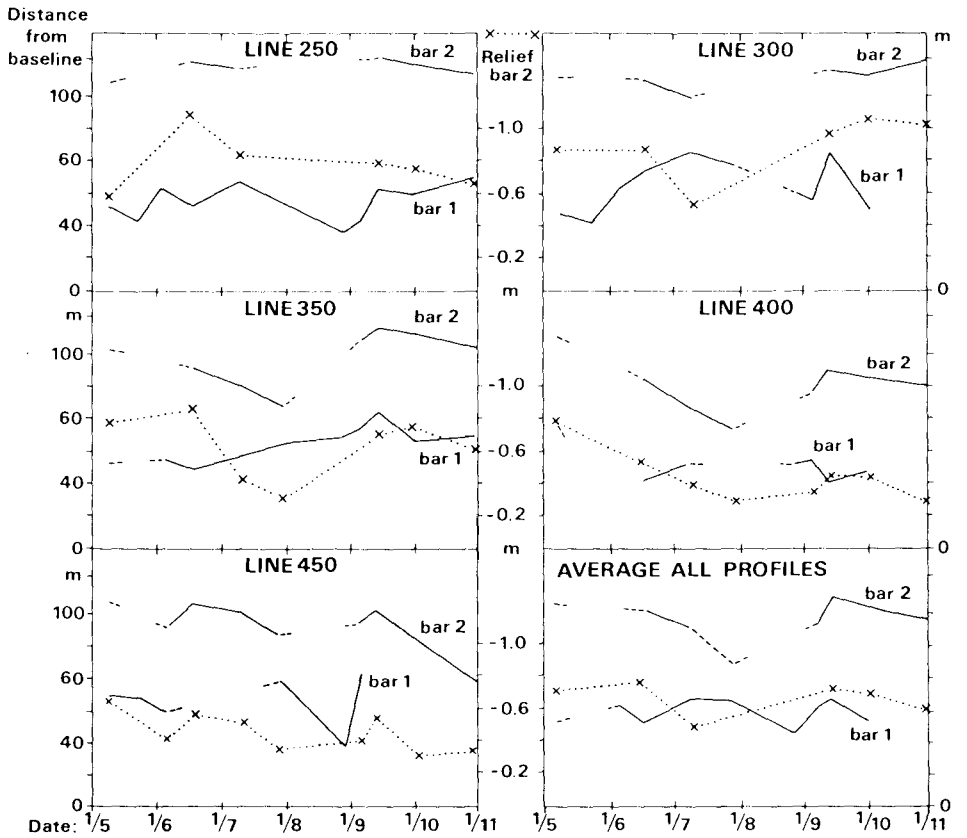

Figure 4. Time/distance diagram of bar crest movement relative to a line of reference on the beach. Dashed or discontinuous lines indicate that the bar was missing, or its position not recorded. Relief of bar 2 is plotted with dots; the magnitude is provided by the right-hand scale.

mum significant incident wave heights were 1.2 m and 0.9 m, respectively. As edge wave amplitude is linearly dependent on the height of the incident waves (GUZA & THORNTON, 1982), it is conceivable that the bar was not moved sufficiently seaward for its position to be in accordance with the edge wave structure; there is a greater morphological inertia in moving a bar as a whole than in developing a crescentic form. Alternatively, the bar may have migrated somewhat shoreward during the period between the "high-energy" event and the survey. Probably both mechanisms were responsible.

Problems arise with the correlation on May 8 and September 5. The greater part of the seaward movement of bar 2 from July 29 - September 5 probably took place on September 4, as the energy level on this day was the highest in the interval. If standing edge waves were involved in causing the bar movement and configuration, the mode number must have been at least 2. But as can be seen from Figure 8 and Table 3, bar 1 is much too far seaward compared to the rhythmic wavelength if this rhythmicity was formed by a mode 2 edge wave. As the storm on September 4 was not very strong, it is conceivable that topographic effects may have played a part in governing the cell circulation leading to the very pronounced rhythmic topography depicted on Figure 5b. On May 8, the bars were situated too far seaward in proportion to the rhythmicity. Thus x_1 and x_2 indicate a hypothetical infragravity wave period of 43-46 seconds, while λ_1 corresponds to a standing edge wave of mode 1 with a period of about 36 seconds. A satisfactory explanation of the bar pat-

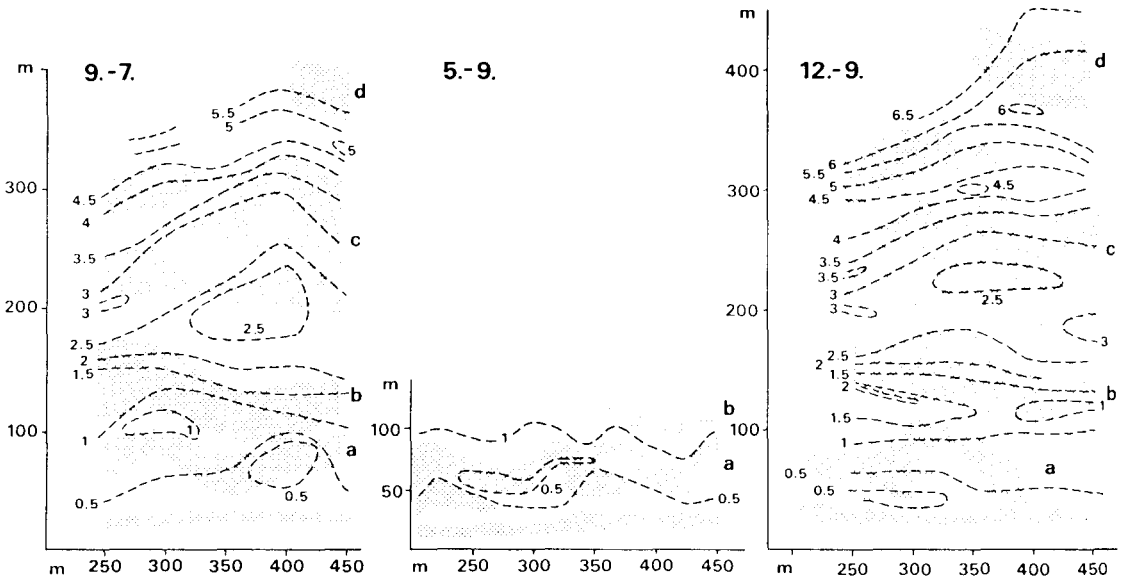

Figure 5. Maps of the study area: July 9, September 5 and 12. Ordinate is offshore and abscissa alongshore distance. Depth contours in metres. Bar 1 = a, bar 2 = b, bar 3 = c, bar 4 = d. Note small swash bars occurring in September. These swash bars were connected to a berm west of the study area and quickly moved shoreward.

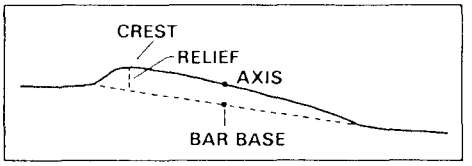

Figure 6. Definitions of employed bar terminology. Bar axis is located at ½ bar width.

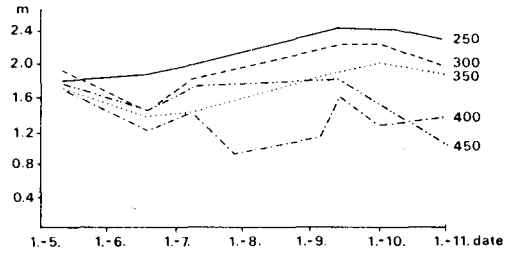

Figure 7. Depth at bar base as a function of time; bar 2. Note that this depth was practically uniform over the study area on May 8, when bar dimensions could not be correlated with an edge wave structure.

Table 2. *Net migration of bar crest between survey dates; bar 2. Figures are in metres. Shoreward migration is positive.*

	Profile lines				
date	250	300	350	400	450
8/5-4/6					+16
4/6-18/6					−15
8/5-18/6	−14	+ 2	+11	+25	+ 1
18/6-9/7	+ 4	+10	+11	+17	+ 4
9/7-29/7			+13	+14	+15
29/7-5/9			−40	−24	− 6
5/9-12/9			− 8	−13	− 9
9/7-12/9	− 5	−17	−35	−23	0
12/9-2/10	+ 4	+ 3	+ 4	+ 4	+17
2/10-29/10	+ 7	− 9	+ 8	+ 5	+26

tern on May 8 cannot be given. On September 12, an excellent correlation existed between periods calculated from eqs. (3) and (6). This case is discussed separately below.

Note that during the summer months, the most likely occurring edge waves were of mode 1 which will not influence the position and morphology of bar 2. This is in line with the fact that bar 1 oscillated back and forth, while bar

Table 3. *Computed standing wave periods on survey dates.* $\bar{\beta}$ *is the mean gradient between the shoreline and the inner edge of bar 2,* $\bar{\beta}_{5m}$ *is the mean gradient between the shoreline and the 5 m contour.* λ_1 *and* λ_2 *are the rhythmic wavelengths of bars 1 and 2;* x_1 *and* x_2 *are the distances from shoreline to bars 1 and 2, with bars at antinodes.*

		T from λ_1 (eq.6), sec.		T from x_1
date	$\bar{\beta}$	n = 1	n = 2	(eq. 3), sec.
8/5	0.0197	36.1	27.9	42.7
18/6	0.0154	55.2	42.8	46.4
9/7	0.0153	67.1	52.0	58.1
29/7	0.0154	60.2	43.9	57.1
5/9	0.0147	46.7	36.2	54.4
12/9	0.0180	53.4	41.3	53.3
2/10	0.0187	50.1	38.8	48.4

		T from λ_2 (eq.6), sec.	T from x_2
date	$\bar{\beta}_{5m}$	n = 2	(eq.3), sec.
8/5	0.0161	30.9	46.1
12/9	0.0171	51.4	52.0

2 generally moved shoreward throughout the summer.

The Storm Event September 6-7 1985

On September 6, a storm suddenly set in at Kattegat. Wind velocity quickly increased to about 25 m/s from northwest; during September 7, the storm slowly waned. Due to instrument failure, wave parameters unfortunately were not registered, but based on previously recorded analogous situations and visual observations, H_b was estimated to have been $\geq$ 2.5 m at the storm peak. It may be mentioned that careful analysis of recorded wave heights reveals that, given a wind direction and speed, the wave height varies within ± 20% at this locality, *i.e.* under a given set of conditions, the wave height generally may be predicted within ± 20%.

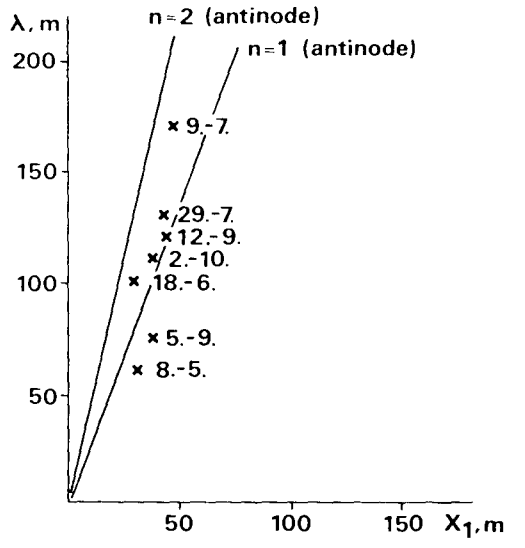

Figure 8. Distance from shoreline to bar 1 (bar axis) plotted against rhythmic wavelength. Points situated along the two lines indicate that bar dimensions are in exact correspondance with the edge wave structure. Cross-shore length scale of the edge wave is assumed similar to the cross-shore structure of a leaky mode standing wave.

The wave period was 6.0 seconds during the afternoon of September 6, while estimated breaker height was 2.5 m. Waves broke 300-350 m from the shoreline (distance estimated from floating buoys) and continued across the wide surf zone as spilling breakers. Conditions were thus fully dissipative.

A pronounced surf beat was observed, periods ranging from 51 to 60 seconds with a mean of 54 seconds (averaged over 20 minutes). The nature of this low-frequency energy could of course not be determined, and the estimate of the period is naturally somewhat subjective.

The beach was severely eroded during the storm. The survey on September 12 showed that the beach had been lowered; generally erosion had taken place on the backshore, deposition on the foreshore and erosion on the inner nearshore, but the tachyometric survey showed that a rhythmic pattern of erosion/deposition appeared on the foreshore/inner nearshore. Zones of deposition were associated with the presence of megacusps and a crescentic bar, Figure 5c. This suggests that standing edge waves were present during or after the storm, as the rhythmic pattern was spatially displaced from September 5 (Figure 5b).

During the period September 5-12, bar 1 migrated seaward in profile lines 250, 300 and 350, while a crescentic horn developed in line 400. Bar 2 also migrated seaward while increasing its relief (Figure 4 and Table 2), while bar 3 did not move significantly. Severe erosion took place on the outer parts of bar 3, where waves broke on September 6, thereby narrowing the bar (Figure 2).

Measurements with depth-of-activity rods (GREENWOOD and HALE, 1980) made by N. Nielsen and J. Nielsen, (Institute of Geography, University of Copenhagen), show that a very large part of the sediment in bars was mobilized

during this storm. Bars were severely eroded and, at least partially, destroyed. An appreciable sediment transport took place, but deposition did not occur throughout the nearshore. After the storm, bars still constituted distinct bands of loose sediment, alternating with morainic material in the troughs. This indicates that the mobilized sediment was redeposited as bars, displaced somewhat seaward from their initial position.

BOWEN (1980) suggested that suspended sediment transport becomes dominant when $u_o/w_s > 15$; u_o being the wave orbital velocity and w_s the sediment fall velocity. u_o was not measured on September 6-7 due to withdrawal of the current meters, but during two somewhat similar situations in October 1984 when H_s reached 1.7 and 2.2 m respectively, orbital velocities over bar 2 reached 0.95 m/s.

The fall velocity of the sediment in the area is about 1. 14 m/s. Taking a conservative value of u_o = 0.95 m/s this gives a u_o/w_s-ratio of about 83, indicating that the greater part of the sediment transport during storms takes place in suspension. According to BOWEN (1980), under such conditions suspended sediment should converge to form bars at antinodes, if standing waves are present.

On September 12, λ_1 was ~ 120 m, while λ_2 was ~ 160 m. The rhythmic wavelength of the bars was confirmed by aerial photographs. With a mean nearshore gradient of a = 0.0171, the rhythmic wavelength of bar 1 corresponds to the half-wavelength of a standing mode 1 edge wave with a period of 55 seconds or the half-wavelength of a mode 2 edge wave with a period of 42 seconds. (Using β = 0. 0180, which was the gradient from the shoreline to the inner edge of bar 2, these periods become 53 and 41 seconds, respectively, Table 3). λ_2 corresponds to the structure of a mode 2 edge wave with a period of 51 seconds, Table 3. As bar 2 moved seaward during the storm, the mode number must have been at least 2, if indeed edge waves were involved in this movement.

Standing wave periods, corresponding to bar distance from the shoreline (measured in the crescentic bays) were 55 seconds and 49 seconds for bars 1 and 2, respectively. However, during the storm peak, water level reached + 1. 16 m DOD. Furthermore, the set-up may be calculated from the theoretical formula

$$\frac{\partial \eta}{\partial x} = \frac{1}{1+(8/3\gamma)^2} \tan\beta \qquad (7)$$

(KOMAR, 1976), where $\partial\eta/\partial x$ is the gradient of the set-up and γ is the breaking criterion, H/h = constant (h is water depth), conventionally put at 0.78. Under dissipative conditions, the value is apparently less than this figure. WRIGHT *et al.* (1982a) found γ = 0.42; SALLENGER and HOLMAN (1985) found γ = 3.2 tan + 0.30; this study indicates $\gamma \sim 0.4$ on September 6, as waves were breaking at a depth of about 6 metres. Alternatively, the set-up may be calculated from the empirical formula

$$\bar{\eta} = 0.17\ H_s \qquad (8)$$

(GUZA and THORNTON, 1981). $\bar{\eta}$ is the set up at the shoreline. As shown by AAGAARD (1986), $H_s \sim H_b$ under high-energy conditions at this locality. Assuming H_s = 2.5 m, γ = 0.4 and x_s = 350 m, eqs. (7) and (8) give set-up values of 0.34 m and 0.42 m, respectively, which gives a total rise of local water level at the shoreline of 1.44 - 1.57 m during the storm peak. Choosing the lower value of 1.44 m, this corresponds to a shoreward displacement of the shoreline of about 18.5 m during the storm, judged from profiles measured on September 12. The standing wave period, corresponding to x_2 in crescentic bays then becomes 52 seconds, in excellent agreement with the value of 51 seconds obtained from λ_2, assuming a mode 2 standing edge wave. Furthermore, these results approximately correspond to periods calculated from the rhythmic pattern of bar 1, assuming a mode 1 edge wave.

During the waning of the storm, water level quickly decreased to 0.35 m DOD, and subsequently levelled off to + 0. 1 m DOD on the day of the survey. A hypothetical interpretation of the succession of events September 6-12 could be that during the storm, edge waves were generated. As bar 2 moved seaward, whereas bar 3 did not show signs of migration, the ratio between distance from shoreline to bars 2 and 3 was 0.55 on September 12, somewhat higher than the theoretical value of 0.48 predicted for bars at antinodes (BOWEN, 1980). Therefore it

is likely that the edge waves had two zero-crossings. Furthermore, the correlation between periods calculated from λ_2 and x_2 indicates mode 2 edge waves.

Whether the edge waves were progressive or standing during the storm peak cannot be determined, but at some point at least, they must have been standing. These edge waves probably caused the location and rhythmic spacing of bar 2, and inferably also of bar 1. In connection with the narrowing of the surf zone and the falling water level associated with the decline of the storm, the mode number may have changed to 1, while the period of the edge waves, T_e, may have remained about the same, thereby changing the position and rhythmicity of bar 1. Morphological evidence suggests that these edge waves may have had periods of 51-55 seconds. Interestingly, the visually observed surf beat on September 6 had a mean period of 54 seconds, but a link between this subjectively estimated surf beat and edge waves cannot be established due to the missing current records.

DISCUSSION

The location of bars after major storms is probably not associated with any breakpoint-controlled mechanism. During the storm on September 6, waves broke far from the shoreline as spilling breakers, and progressed as dissipative bores through the surf zone without any reforming of the waves. No plunging was observed. Under such conditions, the breakpoint hypotheses predict the formation of a single bar at the breakpoint and seaward transport of sediment resulting in bar destruction within the surf zone.

On September 12, two bars were present shoreward of the location of the breaker zone on September 6. The bars had migrated seaward in the period September 5-12; the relief of bar 2 had increased significantly. These observations are not in agreement with the breakpoint hypotheses. Of course the possibility exists that bars 1 and 2 were destructed during the storm, and reformed in the post-storm phase as the breaker zone moved shoreward. However, with a slowly decreasing energy level one would expect the breakpoint to migrate more or less continuously towards the shoreline. Were the formation of bars associated with the position of the breakpoint, one might therefore expect the bars to be of a low and broad appearance. Furthermore, with a breakpoint initially moving seaward in time with the storm intensity, and then shoreward during the decrease of the storm, the nearshore would probably become more or less covered with sand as sediment would have been transported towards the moving breakpoint.

This was not the case after the storm. Bars were, as formerly, appearing as distinct bands upon the compact bottom, although a large part of the sediment had been mobilized during the storm, indicating that sediment transport across the troughs had probably been limited. The position of the troughs remained approximately the same throughout the research period. This suggests a zonation of deposition, independent of the location of the breakpoint.

On September 6, the breaker zone was located over the outer parts of bar 3 where severe erosion was registered after the storm. This fact is also in disagreement with the breakpoint hypotheses.

The nearshore gradient is not uniform throughout the research area; the western part is steeper than the eastern (Figure 5). If bar position was determined by the location of the breakpoint, bar distance from shore might be expected to show an inverse proportionality with the nearshore gradient according to the breaking criterion H/h = constant. Furthermore, as the breaker zone in a given area and under a given set of conditions presumably will be located at a uniform depth (provided that no systematic spatial gradients in H exist, *i.e.* $\partial H/\partial y = 0$) one would expect the bar to be situated at a uniform depth alongshore. This is not the case (Figure 7). Regarding bar 2, depth of bar base as a rule is the largest in line 250, decreasing eastward, reaching a minimum depth in line 400, and again increasing in line 450. This depth varies between 2.25 m (line 250) and 1.5 m (line 400) on September 12.

After the storm, depth of the crest of bar 2 was 1.35 m (line 250), 1. 1 m (line 300), 1. 0 m (line 350), 0.9 m (line 400) and 0.95 m (line 450). These figures are exactly proportional to the values of the nearshore gradient and therefore do not support either breakpoint model as a bar-forming mechanism during the storm on September 6-7.

If the presence of bars were associated with the occurrence of standing infragravity waves,

bars located in the surf zone would accrete during storms as sediment converge towards antinodes (or nodes). This is in accordance with results found in this study. Furthermore, the standing wave hypothesis is able to explain the position of bars in relation to depth and gradient. As x_n with a given standing wave period is proportional to β (eq.2), a given antinode (or node) will be farthest from the shoreline on steep gradients.

The frequent occurrence of approximate identity between edge wave periods computed from rhythmic wavelength and periods computed from bar distance to shore, lends support to the hypothesis of a causal relation existing between standing waves and bar location. Particularly, the correlation was excellent after the storm on September 6-7, where the difference in rhythmic wavelength of bars 1 and 2 could be correlated with the structure of edge waves of the same period, but of differing mode numbers.

The zonation of sediment in distinct shore-parallel bands is equally in accordance with the standing wave model, as zones of deposition and zones of erosion exhibit a crossshore alternation, corresponding to the structure of the standing wave. Figure 8 indicates bar location along offshore antinodes, suggesting that sediment transport should take place in suspension. Considering the small grain size and the significant exceedance of the u_o/w_s threshold ratio during storms, this does seem probable. Implications are that a convergence toward a farther seaward located breaker zone does not take place (perhaps excluding the situation on May 8), but that sand transport is confined within well-defined zones, even when the sand is suspended. These zones may migrate on/offshore depending upon the period and structure of the standing wave.

Of the seven morphologically analyzed situations, four (June 18, July 9, 29, October 2) indicated that standing mode 1 edge waves possibly had influenced the location of bar 1, especially when considering that the bar might have moved somewhat shoreward during the period between the event responsible for the bar location (*i.e.* a "high-energy" situation) and the survey. Alternatively, the bar might not have conformed exactly to the edge wave structure during the "high- energy" situation due to morphological inertia. Results from September 12 show evidence that a standing mode 2 edge wave might have formed bar 2 in connection with the storm, while an ensuing transition of the edge wave to mode 1 of unaltered frequency in the post-storm phase might have reformed bar 1. Twice, on May 8 and September 5, bar position and morphology apparently could not be explained by the standing wave model.

No morphological evidence was found for progressive edge waves or leaky mode standing waves being present. This may be due to the irregular bottom and the bounding headlands which may act as reflectors for progressive edge waves, thus causing these to become standing.

CONCLUSIONS

(1). The movement of the bars displayed a connection with the energy level. Bars migrated seaward during high-energy events and shoreward under lower energy conditions. Bar 2 requires a higher energy level in order to move seaward than bar 1.

(2). The distinct and well-defined bar 2 increases its relief when migrating seaward, and vice versa.

(3). In the chief part of the analyzed situations, a reasonably good correlation was found between bar dimensions and the structure of hypothetically existing edge waves. Almost exact correspondance was found immediately after a storm. Under such conditions, infragravity waves have the greatest possibility of dominating the energy spectrum (GUZA and THORNTON, 1982; GUZA *et al.* , 1985). The difference in rhythmic wavelength of bars 1 and 2 after the storm apparently could be explained as being a result of standing edge waves of identical frequency, but of differing mode numbers. Bar distances from shore were in agreement with the structure of standing infragravity waves with frequencies corresponding to those deducted from the rhythmic pattern.

(4). Due to lack of suitable instruments, the existence of infragravity edge waves with frequencies corresponding to those deducted from the morphology could not be proved.

(5). Bar formation hypotheses mentioned in the literature have been evaluated. The various hypotheses associated with the position of the breaker zone could be rejected, primarily because of the presence and growth of bars in the surf zone during a storm, the non-uniform depth over the bar in a given situation, and the

proportionality between gradient and bar distance from shore. Although the evidence is circumstantial, the existence of standing infragravity waves, probably edge waves, was a likely cause for bar formation and position. During a storm event, these edge waves probably were of mode 2, while mode 1 prevailed under more moderate energy conditions, when the surf zone was narrower.

ACKNOWLEDGEMENTS

I am grateful to J. Nielsen and N. Nielsen for encouragement and constructive criticism during the preparation of this paper. The figures were prepared by J. Jönsson, while N. Larsen and K. Böge assisted in the field. Finally, I would like to express my gratitude to the Danish Hydraulic Institute, especially chief engineer P. Roed Jacobsen, for permission to use and publish their wave and current data.

LITERATURE CITED

AAGAARD, T., 1986. Dynamics and morphology of nearshore bars: A case-study at Hald Strand, North Zealand. Unpubl. M. Sc. Thesis, Univ. of Copenhagen, 187p. (in Danish).

BOWEN, A. J., 1980. Simple models of nearshore sedimentation; beach profiles and longshore bars. IN: S. B. McCann, (Ed.), The Coastline of Canada, *Geological Survey of Canada,* Paper 80-10, 1-11.

BOWEN, A. J. and HUNTLEY, D. A., 1984. Waves, long waves and nearshore morphology. *Marine Geology,* 60: 1-13.

BOWEN, A. J. and INMAN, D. L., 1971. Edge waves and crescentic bars. *Journal Geophysical Research,* 76: 8662-8671.

CARTER, T. G., LIU, P. L. F., and MEI, C. C., 1973. Mass transport by waves and offshore sand bedforms. *Journal Waterways Harbors & Coastal Engineering Division,* 99: 165-184.

DYHR-NIELSEN, M. and SORENSEN, T., 1970. Some sand transport phenomena on coasts with bars. *Proceedings 12th Coastal Engineering Conference,* ASCE, 855-865.

EVANS, O. F., 1940. The low and ball of the eastern shore of Lake Michigan. *Journal of Geology,* 48: 476-511.

EXON, N. F., 1975. An extensive offshore sand bar field in the western Baltic Sea. *Marine Geology,* 18: 197-212.

GREENWOOD, B. and DAVIDSON-ARNOTT, R. G. D., 1975. Marine bars and nearshore sedimentary processes, Kouchibouguac Bay, New Brunswick. IN: J. Hails and A. Carr, (Eds.), *Nearshore Sediment Dynamics and Sedimentation.* London: Wiley, 123-150.

GREENWOOD, B. and DAVIDSON-ARNOTT, R. G. D., 1979. Sedimentation and equilibrium in wave-formed bars: A review and case study. *Canadian Journal Earth Sciences,* 16: 312-332.

GREENWOOD, B. and HALE, P. B., 1980. Depth of activity, sediment flux and morphological change in a barred nearshore environment. IN: S. B. McCann (Ed.), The Coastline of Canada, *Geological Survey of Canada,* Paper 80-10, 89-109.

GREENWOOD, B. and SHERMAN, D. J., 1984. Waves, currents, sediment flux and morphological response in a barred nearshore system. *Marine Geology,* 60: 31-61.

GUZA, R. T. and THORNTON, E. B., 1981. Wave set-up on a natural beach. *Journal Geophysical Research,* 86: 4133-4137.

GUZA, R. T. and THORNTON, E. B., 1982. Swash oscillations on a natural beach. *Journal Geophysical Research,* 87: 483-491

GUZA, R. T., THORNTON, E. B., and HOLMAN, R. A., 1985. Swash on steep and shallow beaches. *Proceedings 19th Coastal Engineering Conference,* ASCE, 708-723

HAYES, M. O., 1972. Forms of sediment accumulation in the beach zone. IN: R. E. Meyer (Ed.), *Waves on Beaches and Resulting Sediment Transport.* New York: Academic Press, 297-356.

HOLMAN, R. A. and BOWEN, A. J., 1982. Bars, bumps and holes: Models for the generation of complex beach topography. *Journal Geophysical Research,* 87: 457-468.

INGLE, J. C., 1966. *The Movement of Beach Sand.* Amsterdam: Elsevier, 221p.

KATOH, K., 1984. Multiple longshore bars formed by long period standing waves. *Report Port Harbour Research Institute,* 23 (3) : 3-46.

KING, C. A. M. and WILLIAMS, W. W., 1949. The formation and movement of sand bars by wave action. *Geographical Journal,* 113: 68-85.

KOMAR, P. D., 1976. *Beach Processes and Sedimentation.* Englewood Cliffs, NJ: Prentice Hall, 429p.

MILLER, R. L., 1976. Role of vortices in surf zone prediction: Sedimentation and wave forces. IN: R. A. Davis and R. L. Ethington (Eds.), Beach and Nearshore Sedimentation, *SEPM Special Publication,* 24: 92-114.

SALLENGER, A. H. and HOLMAN, R. A., 1985. Wave energy saturation on a natural beach of variable slope. *Journal Geophysical Research,* 90: 11939-11944.

SALLENGER, A. H., HOLMAN, R. A., and BIRKEMEYER, W. A., 1985. Storm-induced response of a nearshore-bar system. *Marine Geology,* 64: 237-257.

SALLENGER, A. H., HOWARD, P. C., FLETCHER, C. H., and HOWD, P. A., 1983. A system for measuring bottom profile, waves and currents in the high-energy nearshore environment. *Marine Geology,* 51: 63-76.

SAYLOR, J. H. and HANDS, E. B., 1970. Properties of longshore bars in the Great Lakes. *Proceedings 12th Coastal Engineering Conference,* ASCE, 839-853.

SHORT, A. D., 1975. Multiple offshore bars and stand-

ing waves. *Journal Geophysical Research,* 80: 3838-3840.
SHORT, A. D., 1979. Three-dimensional beach stage model. *Journal Geology,* 87: 553-571.
SVENDSEN, I. A., 1984. Mass flux and undertow in a surf zone. *Coastal Engineering,* 8: 347-365.
URSELL, F., 1952. Edge waves on a sloping beach. *Proceedings Royal Society of London,* A 214: 79-97
WINANT, C. D., INMAN, D. L. and NORDSTROM, C. E., 1975. Description of seasonal beach changes using empirical eigenfunctions. *Journal Geophysical Research,* 80: 1979-1986.
WRIGHT, L. D., CHAPPELL, J., THOM, B. G., BRADSHAW, M. P. and COWELL, P., 1979. Morphodynamics of reflective and dissipative beach and inshore systems: Southeastern Australia. *Marine Geology,* 32: 105-140.
WRIGHT, L. D., GUZA, R. T. and SHORT, A. D., 1982a. Dynamics of a high-energy dissipative surf zone. *Marine Geology,* 45: 41-62.
WRIGHT, L. D., NIELSEN, P., SHI, N. C. and LIST, J. H., 1986. Morphodynamics of a bar-trough surf zone. *Marine Geology,* 70: 251-285.
WRIGHT, L. D., NIELSEN, P., SHORT, A. D., COFFEY, F. C. and GREEN, M. O., 1982b. Nearshore and surfzone morphodynamics of a storm wave environment: Eastern Bass Strait, Australia. *Coastal Studies Unit Technical Report Number 82/3,* Department of Geography, University of Sydney, 154p.